Analytica Chimica Acta 852 (2014) 153–161

Contents lists available at ScienceDirect

Analytica Chimica Acta

journal homepage: www.elsevier.com/locate/aca

Graphene/TiO_2 nanocomposite based solid-phase extraction and matrix-assisted laser desorption/ionization time-of-flight mass spectrometry for lipidomic profiling of avocado (*Persea americana* Mill.)

Qing Shen [1], Mei Yang [1], Linqiu Li, Hon-Yeung Cheung *

Department of Biomedical Sciences, City University of Hong Kong, 83 Tat Chee Avenue, Kowloon,Hong Kong SAR, China

HIGHLIGHTS

- A SPE method using G/TiO_2 as sorbent was developed.
- This method can selectively extract phospholipids from avocado.
- The analytes were detected by MALDI-TOF/MS in positive and negative modes.
- This method is efficient and promising.

GRAPHICAL ABSTRACT

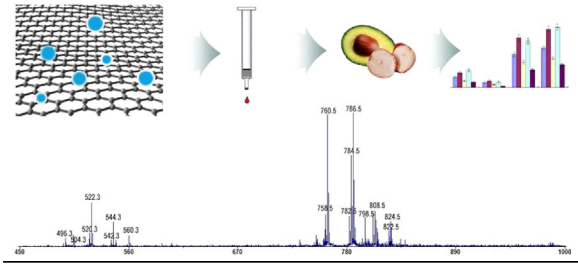

ARTICLE INFO

Article history:
Received 4 June 2014
Received in revised form 10 September 2014
Accepted 11 September 2014
Available online 18 September 2014

Keywords:
Lipidomics
Graphene/TiO_2
Solid-phase extraction
Principal component analysis
MALDI-TOF/MS
Avocado

ABSTRACT

Phospholipids possess important physiological, structural and nutritional functions in biological systems. This study described a solid-phase extraction (SPE) method, employing graphene and titanium dioxide (G/TiO_2) nanocomposite as sorbent, for the selective isolation and enrichment of phospholipids from avocado (*Persea americana* Mill.). Based on the principal that the phosphoryl group in the phospholipid can interact with TiO_2 via a bridging bidentate mode, an optimum condition was established for SPE, and was successfully applied to prepare avocado samples. The extracts were monitored by matrix-assisted laser desorption ionization time-of-flight/tandem mass spectrometry (MALDI-TOF/MS) in both positive-ion and negative-ion modes. Results showed that phospholipids could be efficiently extracted in a clean manner by G/TiO_2 based SPE. In addition, the signals of phospholipids were enhanced while the noise was reduced. Some minor peaks became more obvious. In conclusion, the nanocomposite material of G/TiO_2 was proved to be a promising sorbent for selective separation of phospholipids from crude lipid extract.

1. Introduction

Persea americana Mill. (family: Lauraceae), commonly known as 'avocado', is a tropical and subtropical fruit. Although *P. americana* is a native plant in Central America (Mexico), it grows in places as far from America, Australia, South Africa, and so on. Avocados are rich in unsaturated fatty acids, folic acid, dietary fiber, vitamins, pantothenic acid, and other nutrients [1]. Lipophilic extract of avocado has been revealed be potent in lowering risk of cardiovascular and diabetes, attenuating liver injury, inhibiting prostate cancer cell growth, and inducing apoptosis in human

Abbreviation: PC, phosphatidylcholine; PE, phosphatidylethanolamine; PI, phosphatidylinositol; PA, phosphatidic acid; PG, phosphatidylglycerol; G/TiO_2, graphene/titanium dioxide nanocomposite; B&D, Bligh & Dyer; MALDI-TOF/MS, matrix-assisted laser desorption ionization-time of flight/mass spectrometry; PCA, principal component analysis.

* Corresponding author. Tel.: +86 852 34427746; fax: +86 852 34427406.
E-mail address: bhhonyun@cityu.edu.hk (H.-Y. Cheung).

[1] These authors contributed equally to this work.

http://dx.doi.org/10.1016/j.aca.2014.09.022

breast cancer cells [2–5]. The consumption of avocado in United States has increased in recent years, and it amounted up to 740,000 t in 2013. However, seeds, peels, and other parts are normally discarded as useless when consuming or processing, causing environmental waste problems. Recovery of bioactive plant constituents from food industrial waste is promising and will be a cost-effective and environmental friendly option.

Phospholipids (PLs) are the primary structural constituents of biological membranes, possessing important physiological functions and positive nutritional properties. The molecular types of phospholipids varied greatly due to a glycerol backbone with one headgroup at the sn-3 position and a fatty acyl substituent at the sn-1 and/or sn-2 position. They have been reported to exert beneficial effects on human health, such as anti-inflammatory activity and reduction of the risk of cardiovascular disease [6,7]. Furthermore, PLs have been recognized as potential biomarkers for ovarian cancer, diabetes, and other diseases [8–11]. Recently, driven by the rapid advances in technologies such as mass spectrometry (MS), a new concept, namely lipidomics, has been used to describe the complete lipid profile within a cell, tissue, or organism on a large-scale and at the intact-molecule level. MS based lipidomics profiling efficiently generates qualitative, quantitative, and reproducible analytical results from any environmental, clinical, biological or food samples [12–17]. However, there are still challenges in the PLs analysis, which are arisen from the low abundance of nonpolar triglycerides, and the simultaneous occurrence of a number of positional and structural isomers.

Graphene has attracted increasing interest for both fundamental science and applied research, due to its unique two-dimensional double-sided structure [18]. Integrating graphene with other inorganic materials to fabricate composites or hybrids is the focus of the applications. The high specific surface area and loading capacity endows graphene a good support to achieve a uniform distribution of the loaded nanoparticles. Meanwhile, TiO_2 is reported as an ideal material for separation and enrichment of phosphorylated compounds [19]. It has already been comprehensively used to selectively extract phophopeptide from crude mixture [20]. Recently, endeavors have been devoted to exploit TiO_2 as affinity material for extraction of phospholipids [21,22]. The mechanism behind involves two distinct binding modes between phosphopeptides or phospholipids and TiO_2. The hydroxyl groups in phosphopeptides and some phospholipid classes, like PA and PI, bind via a chelating bidentate mode, while the phosphoryl group binds through a bridging bidentate mode [23].

In this report, we integrate graphene and TiO_2 and use this nanocomposite as SPE sorbent for the purification and enrichment of phospholipids from avocado. Both the pulp and seed of avocado were tested. The fortified phospholipid samples were further subjected to fast MALDI-TOF/MS for profiling. The overall method was optimized.

2. Materials and methods

2.1. Materials

Avocados were purchased from local market and well stored in the Laboratory of Natural Products, City University of Hong Kong. For preparation, all avocado samples were separated into two parts, pulps and seeds. 2,5-dihydroxybenzoic acid (DHB) and 9-aminoacridine (9AA) were purchased from Sigma–Aldrich (St. Louis, MO, USA). HPLC grade chloroform and methanol were purchased from Fisher Scientific (Waltham, MA, USA). Water with a resistivity of 18 MΩ cm was purified by a Milli-Q system from Millipore (Billerica, MA, USA). Other chemicals and solvents used were in the highest quality without additional purification unless specified otherwise.

2.2. Synthesis of G/TiO_2 nanocomposite

Graphite oxide (GO) was synthesized by an improved Hummer's method [24], a 9/1 mixture of concentrated H_2SO_4/H_3PO_4 (360 mL/40 mL) was added to a mixture of graphite flakes (3.0 g, 1 wt equiv.) and $KMnO_4$ (18.0 g, 6 wt equiv.), producing a slight exotherm to ca. 40 °C. The reaction mixture was then heated to 50 °C and stirred for 12 h. The reaction mixture was cooled to room temperature and poured onto ice (ca. 400 mL) and quenched with 30% H_2O_2 (5 mL). For workup, the mixture was neutralized by three cycles of centrifuged (10,000 rpm for 2 h), decantation, and suspension in 4 wt% aqueous HCl solution. The remaining solid material was then dialyzed in ultrapure deionized water to remove remaining salts (4 × 5 L, with water changed every 4 h during daytime or after overnight). The solid was collected and vacuum-dried overnight at room temperature, obtaining 5.6 g of product.

G/TiO_2 hybrid was synthesized in a previously reported two-step way [25]. Briefly, 16.0 mg of GO was dissolved in EtOH/water (350 mL/25 mL). The suspension was heated to 80 °C under water bath with stirring. Then a solution of $Ti(BuO)_4$ (0.9 mL) and H_2SO_4 (0.375 mL) in 25 mL of EtOH was added and the mixture was kept continuously stirring at 80 °C for 12 h. Then, the reaction mixture was cooled down and the composite was collected by centrifugation and then washed with water for several times. In the second step of the synthesis, the washed composite was dispersed in water/DMF (125 mL/2.5 mL). The suspension was transferred to a 200 mL Teflon-lined stainless steel autoclave for hydrothermal reaction at 200 °C for 24 h. The final product was collected by centrifugation and then washed with water. Fig. 1 shows the SEM scanning images of graphene and G/TiO_2 nanocomposite. As shown in Fig. 1A, the surface of graphene was smooth. After the

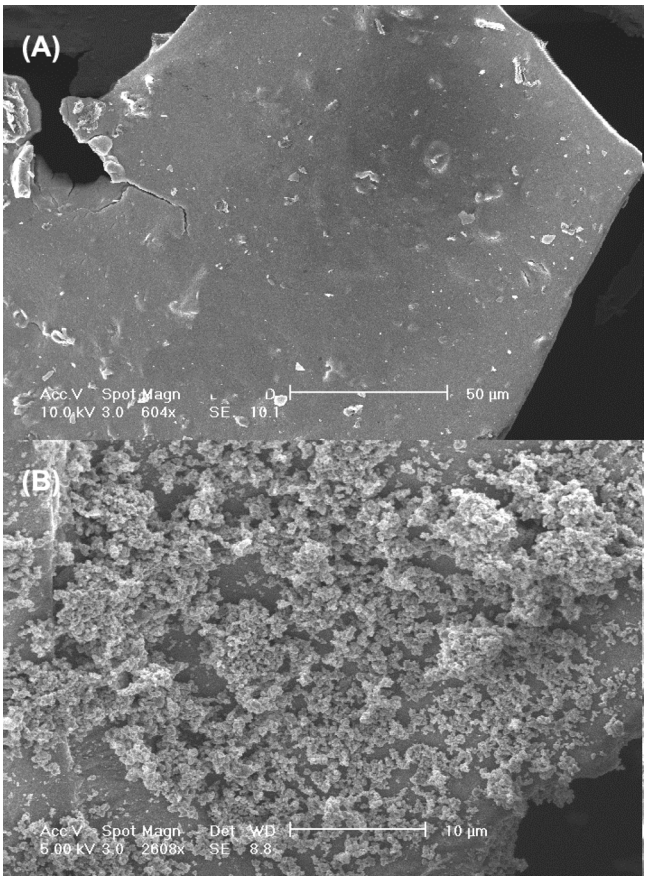

Fig. 1. SEM image of (A) graphene; (B) G/TiO_2 nanocomposite.

TiO_2 coating, the surface of graphene was covered with TiO_2 particles (Fig. 1B). TEM image showed that the size of TiO_2 particle is around 20 nm (Fig. S1).

2.3. Sample preparation

Crude lipids were extracted using classic Bligh & Dyer (B&D) method. Briefly, approximate 1.0 g of homogenized sample was mixed with 1.75 mL binary solvent mixture of chloroform and methanol (1:2, v/v). Then, sample mixture was added with 1.25 mL chloroform and followed by sonication extraction for 15 min. After that, an aliquot of 1.25 mL water was added to separate the solvent phases. The mixture was centrifuged at 8000 rpm for 10 min, and the lower organic phase was transferred to a new glass tube by micropipette. The aqueous phase was re-extracted with 2.0 mL chloroform for another two times as described before. The collected organic phases were combined, evaporated under nitrogen flow, re-dissolved in methanol, and diluted with water.

2.4. SPE preparation

A mass of 100 mg G/TiO_2 nanocomposite was packed into a 1 mL cartridge. Polypropylene materials were set as frits at the both sides to hold the sorbent (obtaining a bed of 0.6 cm height of G/TiO_2). Before use, the SPE was preconditioned by washing with 3.0 mL methanol and activated with 3 mL water (pH 5). Then, the crude extract was loaded and passed through the cartridge at a flow rate of 0.5 mL min^{-1}. Subsequently, the cartridge was washed with cold acetone to remove nonpolar compounds. Then, analytes retained on the SPE sorbent were eluted with 3 mL mixture of chloroform and methanol (1:2), and the eluent was then analyzed by MALDI-TOF/MS. For methods comparison, two previously reported methods were also tested, and the detailed procedure is given in Supplementary materials.

2.5. MALDI-TOF/MS

Applied Biosystems 4800 MALDI-TOF mass spectrometer (AB Sciex, Foster City, CA) was used for lipid analysis, equipped with a 200 Hz tripled-frequency Nd:YAG pulsed laser with 355 nm wavelength. Assays were conducted in both positive and negative ion reflection mode at an accelerating potential of 20 kV. A delayed ion extraction time of 450 ns was selected according to the mass range under observation (m/z 450–1000) allowing for baseline isotopic mass resolution. Mass spectra were obtained by applying laser energy adjusted up to 5–10% above threshold irradiation according to the manufacturer's nominal scale. The sample spots under investigation was directly observed by an integrated video imaging system at about 25 fold magnification. External mass calibration was achieved using mixture of phospholipid standard chemicals. MS data was acquired by 4000 Series Explorer, version 3.5.2 program. An isotopic correction was conducted to confirm that minor peaks were not originated from the isotopic distribution of the adjacent and the more dominant lipid peaks.

2.6. Data analysis

MALDI-TOF/MS data was analyzed by the supplied instrument software Data Explorer v.4.9 (Applied Biosystems) using the Savitzky–Golay smoothing algorithm. Characterization of lipid was performed by comparing accurate mass information with the LIPID MAPS prediction tool (http://www.lipidmaps.org/tools/index.html) and confirmed by MS/MS in the LIFT-TOF/TOF mode. Values were represented as mean ± standard deviation (SD) of at least triplicate measurements ($n \geq 3$). Principal component analysis (PCA) was applied to determine the main variability presented in the data sets, and to establish the relation between samples (objects) and phospholipids (variables). The raw data were imported into the statistical software package MarkerView, version 1.2.1 (AB Sciex, Concord, Canada), and the difference in the mass fragments (m/z) and the relative abundance could be obtained.

3. Results and discussion

3.1. Optimization of SPE

In order to evaluate the analytical potential of G/TiO_2 as SPE sorbent, and to obtain extracts with high recovery and low effect of matrix interferences from the avocado samples, effects of different parameters (pH of sample, type of washing solution and volume of eluent) on the abundance of phospholipids were investigated. PC (14:0/14:0), PE (15:0/15:0), PA (14:0/14:0), PG (15:0/15:0) and PI (16:0/16:0) were adopted as model compounds. It should be pointed out that the selected conditions were a compromise resulting from the chemically diverse set of phospholipids. These conditions may be far from optimal for some compounds.

3.1.1. pH of sample

The pH of sample, adjusted from 2 to 9, was applied to remove the polar compounds and enhance the binding ability of the G/TiO_2

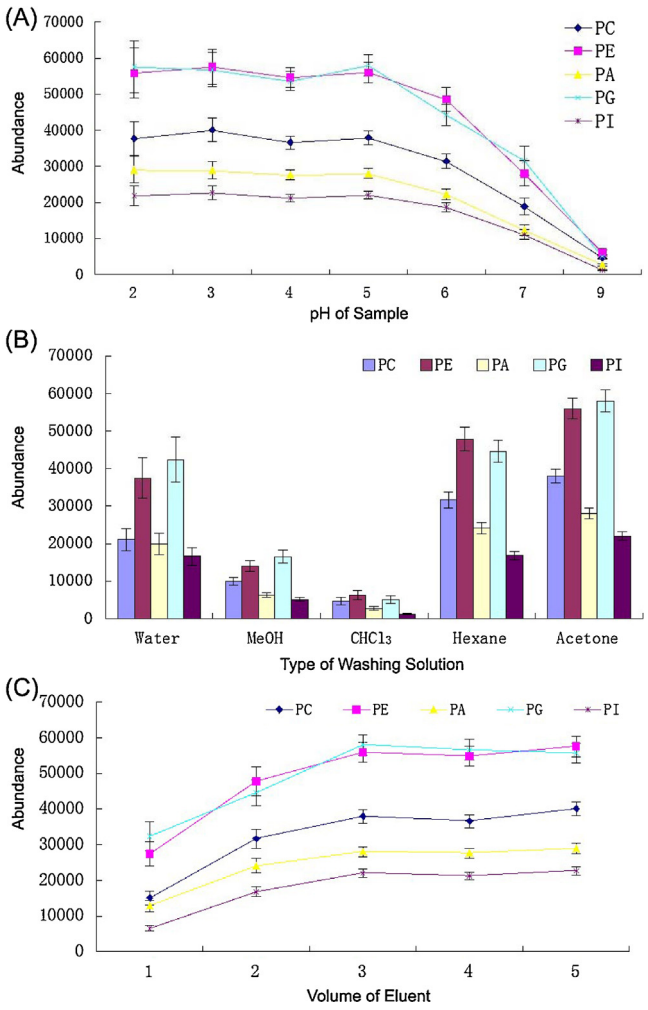

Fig. 2. Effect of (A) pH of sample, (B) type of washing solution (cold acetone), (C) volume of eluent (chloroform/methanol, 1/2), on the efficiency of G/TiO_2 based SPE technique.

sorbent. The results are shown in Fig. 2A. When pH increased from 2 to 5, the abundance of phospholipids was not changed significantly. If extreme acidic condition (pH from 2 to 3) was used, the results became unstable as revealed by the standard deviation (SD). When the sample was adjusted to neutral or even basic, the abundance of phospholipids decreased gradually. Considering these results, the pH of the crude sample was adjusted to pH 5 before loading.

3.1.2. Type of washing solution

For the washing solution, it should efficiently help to remove as much as interfering matrix from the cartridge but retain the target analytes on the sorbent. In order to eliminate the glycerides in avocado samples, the cartridges were subjected to washing solvents of water, methanol, chloroform, hexane, and acetone, respectively. As observed in Fig. 2B, methanol and chloroform were unsuitable to be used as washing solutions, because they induced loss of a large amount of phospholipids. Water improved the abundance of phospholipids, but the nonpolar matrix could not be effectively removed. The performance of both hexane and acetone were satisfactory. The latter one was selected as washing solution, as it generated the highest abundance of phospholipids in a clean manner. Meanwhile, the cartridge was easier to be dried due to the high volatility of acetone.

3.1.3. Volume of eluent

After the washing step, to desorb specifically the target analytes in the cartridge, the SPE was followed by an elution step with an appropriate amount of eluent. The volume of eluent, ranged from 1 mL to 5 mL, was tested in this study. For all the tested phospholipid standards (Fig. 2C), the extraction efficiency increased along with an increase of elution volume. The highest abundance of phospholipids was obtained at an elution volume of 3 mL, and no improvement was observed with a further increase of elution volume. Therefore, 3 mL was enough for eluting the phospholipids from the SPE sorbent.

3.2. Method development and lipid characterization

According to preliminary experiment, DHB and 9AA were selected as the matrix for positive ion mode and negative ion mode, respectively, as they can be easily dissolved in organic solvents. This property efficiently helps to enhance the homogeneity of the crystallization of the matrix and sample. Therefore, the reproducibility of MALDI-TOF/MS data acquisition and the resolution of mass spectra can be increased [26]. B&D method was used as a starting point in this part of study, since, it was one of the most wildly used technique for extracting polar lipids. Fig. 3A reports the MALDI-TOF/MS spectrum relevant to the B&D extract of avocado

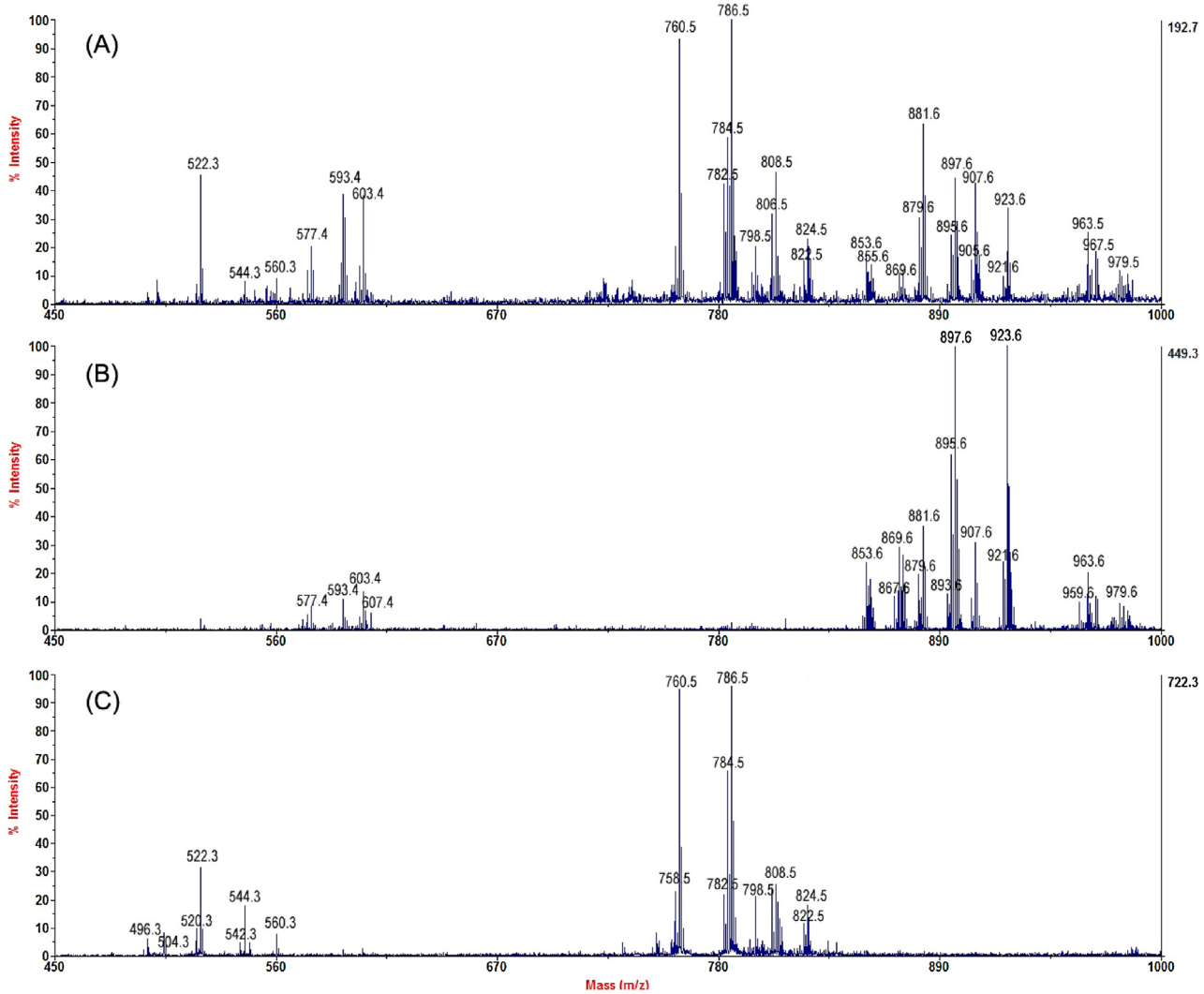

Fig. 3. Positive MALDI-TOF/MS spectra relevant to the extracts of avocado pulp sample by using (A) B&D method; (B) acetone as washing solution for pretreatment; (C) eluate from G/TiO_2 SPE cartridge.

pulp sample in the positive ion mode. As shown, two groups of lipids were observed, one was glycerides in the *m/z* range of 850–950, and the other was phospholipids in the *m/z* range of 750–850 and 450–550.

For SPE strategy, the crude B&D extract was loaded on the G/TiO_2 sorbent and the SPE cartridge was washed with acetone under the optimized conditions. The obtained washing solution was also analyzed by MALDI-TOF/MS technique. As demonstrated in Fig. 3B, the glycerol ions were observed in a clean manner, indicating that acetone removed the nonpolar lipids well from the SPE cartridge and could be regarded as a good washing solution. For characterization, the dominate peaks were identified as TAG in the *m/z* range of 850–950. The potassium adducts of TAG, i.e., $[TAG+K]^+$, were the majority proportion, while sodium adducts of TAG were the minor with lower intensities. The dominate peaks identified in the TAG region were $[POO+Na]^+$ (*m/z* 881.6), $[POO+K]^+/[PSL+K]^+$ (*m/z* 897.6), $[OOO+Na]^+/[SOL+Na]^+$ (*m/z* 907.6), $[OOO+K]^+/[SOL+K]^+$ (*m/z* 923.6), and $[POL+Na]^+$ (*m/z* 879.6) (Table S1). Other major ion peaks were confirmed as $[POP+Na]^+$ (*m/z* 855.6), $[POL+K]^+$ (*m/z* 895.6), as well as sodium adducted components $[OOL+Na]^+$ (*m/z* 905.6), $[SLB+Na]^+/[OOB+Na]^+$ (*m/z* 963.5), $[SSB+Na]^+$ (*m/z* 967.5), etc. The fragments of $[TAG+K/Na]^+$ ions that lost a fatty acyl moiety as well as the $[DAG+K/Na]^+$ ions were observed in the mass range of *m/z* 550–650, in which the dominant DAG ions of *m/z* 577.4, 593.4, and 603.5 were corresponded to fragment ions $[PO]^+$, $[LLN]^+$, and $[OO]^+$, respectively. All the detectable glycerol ions were tabulated in Table S1.

The eluate from G/TiO_2 based SPE cartridge is illustrated in Fig. 3C. Phospholipids, as one of the important lipid group, were observed with abounding quantities. Based on MS/MS data, literature reports and database LIPID MAPS, peaks obtained in the *m/z* range of 750–850 and 450–550 were identified as phospholipids and lysophospholipids, respectively. PC species adducted with hydrogen, potassium or sodium were the dominant ions, while PE species were detected in minor abundance. Due to positive charge, quaternary ammonia groups of the former enable specific detection of PC species. Dominant PC species accompanied with moderately unsaturated oleic acyl and linoleic acyl residues were identified as $[PC16:0/18:1+H]^+$ (*m/z* 760.5), $[PC18:2/18:2+H]^+$, $[PC16:0/18:1+Na]^+$ (*m/z* 782.5), $[PC18:1/18:2+H]^+$ (*m/z* 784.5), and $PC18:0/18:2+H]^+$ and $[PC18:1/18:1+H]^+$ (*m/z* 786.5). In this report, no highly unsaturated fatty acyl residues such as docosahexaenoyl (22:6) and eicosapentaenoyl (20:5) were detected. This is greatly different from the aquatic organisms. Moreover, potassium or sodium adducted compositions such as $[PE18:1/22:2+H]^+$ and $[PE18:0/20:0+Na]^+$ (*m/z* 798.5), $[PC18:0/18:2+Na]^+$, $[PC18:1/18:1+Na]^+$ (*m/z* 808.5), $[PC18:1/18:2+Na]^+$ (*m/z* 806.5), $[PC18:1/18:2+K]^+$ (*m/z* 822.5) as well as $[PC18:0/18:2+K]^+$ and $[PC18:1/18:1+K]^+$ (*m/z* 824.5) were also detected at a high relative level. In the *m/z* range of 470–570,

Table 1
Attribution of the main phospholipid ions observable in the spectra of Fig. 3C (positive-ion mode) and Fig. 4B (negative-ion mode), and Fig. 5B (positive-ion mode) and Fig. 5 C (negative-ion mode).

Mass (*m/z*)	Probable attribution	Pulp	Seed	Mass (*m/z*)	Probable attribution	Pulp	Seed
Positive-ion mode				Negative-ion mode			
732.5	$[PC16:0/16:1+H]^+$	1.24 ± 0.26	–	671.4	$[PA16:0/18:2-H]^-$, $[PA16:1/18:1-H]^-$	–	3.88 ± 1.09
736.5	$[PE18:3/18:3+H]^+$	–	1.05 ± 0.22	673.4	$[PA16:0/18:1-H]^-$	–	3.56 ± 1.03
738.5	$[PE18:2/18:3+H]^+$	–	1.25 ± 0.38	695.4	$[PA18:1/18:3-H]^-$	0.42 ± 0.07	3.14 ± 0.54
747.5	$[PG16:1/18:1+H]^+$	0.61 ± 0.10	–	697.4	$[PA18:1/18:2-H]^-$	1.03 ± 0.23	3.82 ± 0.83
749.5	$[PG16:0/18:1+H]^+$	1.81 ± 0.31	–	699.4	$[PA18:0/18:2-H]^-$, $[PA18:1/18:1-H]^-$	0.56 ± 0.08	2.41 ± 0.55
754.5	$[PC16:1/18:3+H]^+$	–	1.10 ± 0.33	712.5	$[PE16:1/18:2-H]^-$	0.83 ± 0.25	–
756.5	$[PC16:1/18:2+H]^+$, $[PC16:0/18:3+H]^+$	2.04 ± 0.64	1.57 ± 0.36	714.5	$[PE16:0/18:2-H]^-$	1.01 ± 0.28	3.26 ± 0.68
758.5	$[PC16:0/18:2+H]^+$	5.65 ± 1.28	11.80 ± 2.96	716.5	$[PE16:0/18:1-H]^-/[PE16:1/18:0-H]^-$	1.08 ± 0.17	1.40 ± 0.30
760.5	$[PC16:0/18:1+H]^+$	21.06 ± 4.64	12.77 ± 2.33	721.5	$[PG16:0/16:0-H]^-$	0.56 ± 0.14	1.20 ± 0.32
778.5	$[PC16:1/18:2+Na]^+$	–	1.48 ± 0.23	738.5	$[PE18:2/18:2-H]^-$, $[PC16:1/18:3-CH_3]^-$	2.09 ± 0.42	2.32 ± 0.69
780.5	$[PC18:2/18:3+H]^+$, $[PC16:0/18:2+Na]^+$	0.63 ± 0.16	3.64 ± 0.50	740.5	$[PE18:1/18:2-H]^-$, $[PC16:1/18:2-CH_3]^-$	2.85 ± 0.82	2.27 ± 0.39
782.5	$[PC18:2/18:2+H]^+$, $[PC16:0/18:1+Na]^+$	4.54 ± 0.73	9.84 ± 1.98	742.5	$[PE18:1/18:1-H]^-$, $[PC16:0/18:2-CH_3]^-$	1.74 ± 0.52	1.73 ± 0.34
784.5	$[PC18:1/18:2+H]^+$	13.97 ± 2.61	16.01 ± 3.65	744.5	$[PE18:0/18:1-H]^-$, $[PC16:0/18:1-CH_3]^-$	1.25 ± 0.25	1.62 ± 0.49
786.5	$[PC18:0/18:2+H]^+$, $[PC18:1/18:1+H]^+$	21.31 ± 5.49	7.95 ± 1.21	745.5	$[PG16:0/18:2-H]^-$, $[PG16:1/18:1-H]^-$	0.78 ± 0.18	1.06 ± 0.32
788.5	$[PC18:0/18:1+H]^+$	0.71 ± 0.17	–	747.5	$[PG16:0/18:1-H]^-$	1.72 ± 0.42	1.85 ± 0.42
796.5	$[PE18:1/20:0+Na]^+$	0.59 ± 0.12	4.00 ± 0.82	766.5	$[PE18:1/20:3-H]^-$, $[PE18:2/20:2-H]^-$, $[PC18:2/18:2-CH_3]^-$	–	–
798.5	$[PE18:1/22:2+H]^+$, $[PE18:0/20:0+Na]^+$	1.71 ± 0.44	6.74 ± 1.41	767.5	$[PG18:2/18:3-H]^-$	–	–
800.5	$[PE18:1/22:1+H]^+$, $[PE18:0/22:2+H]^+$	0.55 ± 0.11	1.08 ± 0.18	768.5	$[PE18:1/20:2-H]^-$, $[PE18:2/20:1-H]^-$, $[PC18:1/18:2-CH_3]^-$	1.62 ± 0.28	0.88 ± 0.19
804.5	$[PC18:2/18:2+Na]^+$	–	1.60 ± 0.46	815.6	$[PI\ O\text{-}16:1/18:3-H]^-$	2.42 ± 0.60	–
806.5	$[PC18:1/18:2+Na]^+$	0.50 ± 0.11	3.40 ± 0.65	817.6	$[PI\ O\text{-}16:1/18:2-H]^-$	4.24 ± 0.78	3.50 ± 0.89
808.5	$[PC18:0/18:2+Na]^+$, $[PC18:1/18:1+Na]^+$	0.92 ± 0.20	2.59 ± 0.42	819.5	$[PI\ O\text{-}16:1/18:1-H]^-$	12.00 ± 3.83	6.39 ± 2.11
810.5	$[PC18:0/18:1+Na]^+$	0.95 ± 0.18	–	821.5	$[PI\ O\text{-}16:0/18:1-H]^-$	0.43 ± 0.07	0.86 ± 0.20
814.5	$[PC18:1/20:1+H]^+$	0.53 ± 0.15	–	831.5	$[PI16:1/18:2-H]^-$	2.59 ± 0.74	3.33 ± 0.84
820.5	$[PC18:2/18:2+K]^+$	–	2.87 ± 0.79	833.5	$[PI16:0/18:2-H]^-$, $[PI16:1/18:1-H]^-$	10.08 ± 2.21	15.26 ± 2.29
822.5	$[PC18:1/18:2+K]^+$	1.05 ± 0.35	5.78 ± 1.70	835.5	$[PI16:0/18:1-H]^-$	8.25 ± 1.88	6.71 ± 1.77
824.5	$[PC18:0/18:2+K]^+$, $[PC18:1/18:1+K]^+$	1.66 ± 0.22	3.50 ± 1.06	843.6	$[PI\ O\text{-}18:1/18:3-H]^-$	2.95 ± 0.53	2.50 ± 0.70
				845.6	$[PI\ O\text{-}18:1/18:2-H]^-$	11.30 ± 2.46	2.48 ± 0.42
				847.6	$[PI\ O\text{-}18:1/18:1-H]^-$; $[PI\ O\text{-}18:0/18:2-H]^-$	0.67 ± 0.10	–
				857.6	$[PI16:0/18:0-H]^-$	0.52 ± 0.14	0.87 ± 0.25
				859.5	$[PI18:0/18:3-H]^-$, $[PI18:1/18:2-H]^-$	1.28 ± 0.31	1.39 ± 0.41
				861.6	$[PI18:0/18:2-H]^-$, $[PI18:1/18:1-H]^-$	1.28 ± 0.33	0.88 ± 0.26

lysophospholipids, including ions of *m/z* 520.3 and 522.3, were detected and identified as $[LPC18:2+H]^+$ and $[LPC18:1+H]^+$, respectively. All the detectable phospholipid ions and lysophospholipids are tabulated in Table 1 and Table S2, respectively.

In this report, negative ion mode was conducted. The acidic phospholipids were more sensitively detected as negative ions in the sample with excess of PC or sphingomyelin [27]. MALDI-TOF spectra of avocado pulp sample showed more diversity than that in the positive ion mode. Some class of phospholipids, such as PI, PG, PA, and PE, are more sensitively and accurately detectable in the negative ion model. As shown in Fig. 4A (B&D method) and B (G/TiO_2 method), about 58–80% of the total phospholipids were counted as the PI species. In the zoomed *m/z* range of 800–870 (Fig. 4C), the most abounding peaks were identified as [PI O-16:1/18:1 – H]$^-$ (*m/z* 819.6), [PI 16:0/18:2 – H]$^-$/[PI 16:1/18:1 – H]$^-$ (*m/z* 833.5), [PI 16:0/18:1 – H]$^-$ (*m/z* 835.5), and [PI O-18:1/18:2 – H]$^-$ (*m/z* 845.5), etc. (Table 1). In the mass range of 650–800 (Fig. 4D), part of the phospholipids were identified as PC and PE, which were together counted for 9–15%. Without LC separation of lipid classes, some ion fragments of PC species $[M-CH_3]^-$and PE species $[M-H]^-$ were overlapped in the negative-ion mode of MALDI-TOF/MS. For example, ions of $[PC16:1/18:3-CH_3]^-$ and [PE18:2/18:2 – H]$^-$ were overlapped at *m/z* 738.5, while peaks of $[PC16:1/18:2-CH_3]^-$ and [PE18:1/18:2 – H]$^-$ were simultaneously detected at *m/z* 740.5. Ions of *m/z* 742.5 was identified as [PE18:1/18:1 – H]$^-$ or [PC16:0/18:2 – CH3]$^-$. For the peak detected at 768.5, ions of $[PC18:1/18:2-CH_3]^-$, [PE18:1/20:2 – H]$^-$, and [PE18:2/20:1 – H]$^-$ were identified. Other majority ions in the *m/z* range of 650–800 were identified as PA and PG, like [PA18:0/18:2 – H]$^-$ or [PA18:1/18:1 – H]$^-$ (*m/z* 699.4) and [PG16:0/18:1 – H]$^-$ (*m/z* 747.5). As observed in Table 1, PA and PG only accounted for about 10% of the total phospholipids. The limited amount of PA and PG could be

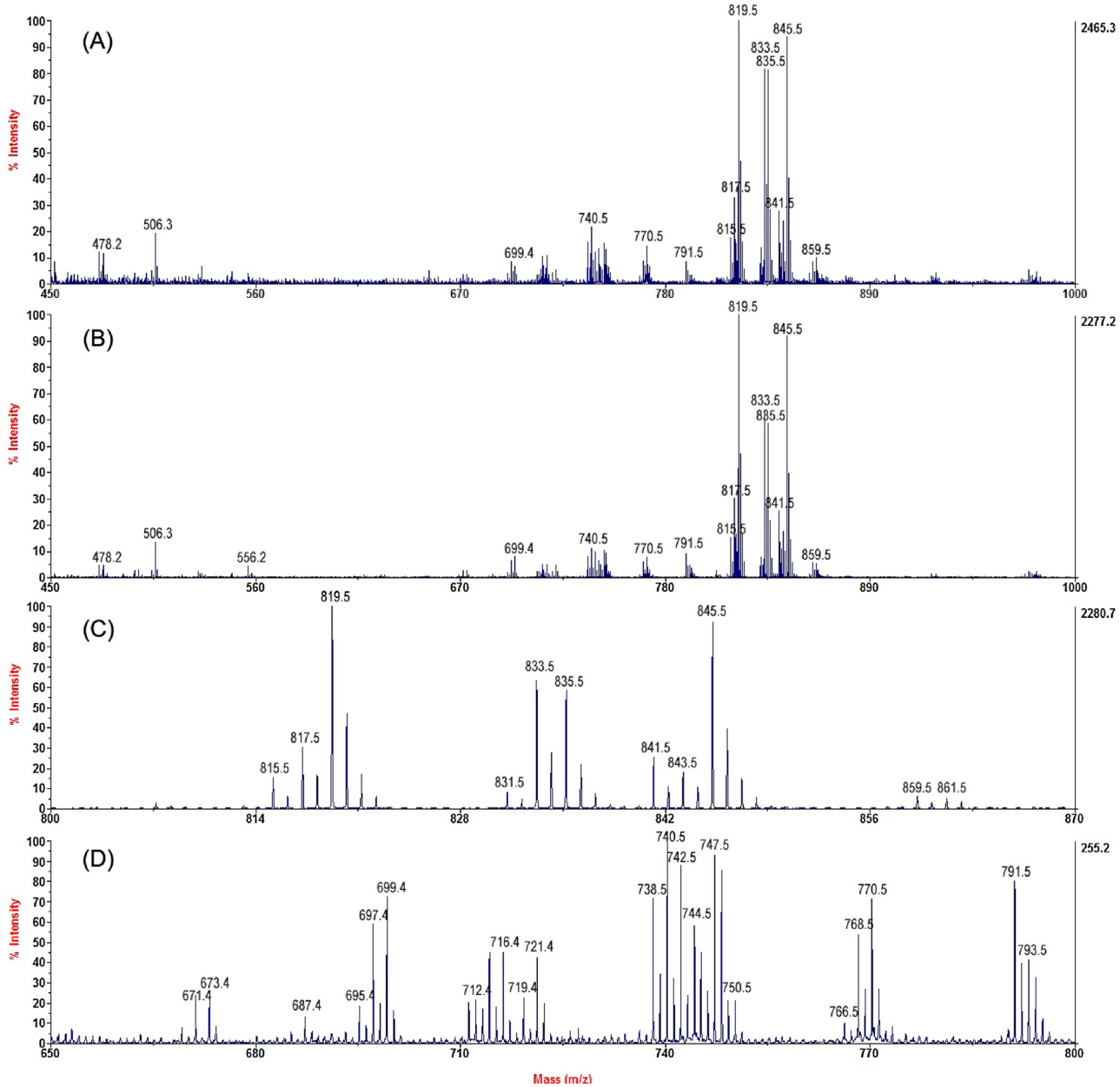

Fig. 4. Negative MALDI-TOF/MS spectra relevant to (A) B&D extracts and (B) G/TiO_2 based SPE extracts of avocado pulp sample. Zoom of the *m/z* range (C) 800–870 and (D) 650–800.

partially attributed to the following reasons: (1) PA mainly functioned as signaling molecule, and some of which could be converted to triglycerides; (2) the process of PG synthesis via cytidine diphosphate-diacylglycerol myoinositol phosphatidyltransferase from phosphatidate could be suppressed by the process of PI synthesis [28].

The crude lipid extract of seed was also subjected to the G/TiO_2 based SPE technique. The spectrum of B&D method was composed by the signals of glycerides and phospholipids (Fig. 5A), while that of G/TiO_2 method was quite clean and only phospholipids could be observed (Fig. 5B). The spectrum of G/TiO_2 method in negative ion mode was also tested and shown in Fig. 5C. Since the species of phospholipids in seeds were generally similar with that in pulps, the characters of phospholipids can be found in the previous section and is not discussed here.

3.3. Method comparison

Lipid profiles of avocado pulp sample obtained from both B&D method and G/TiO_2 nanocomposite based SPE method were comprehensively compared by MALDI-TOF/MS technique. Meanwhile, performance of G/TiO_2 based SPE method was also compared with that of other reported techniques, such as TiO_2 based matrix solid-phase dispersion (MSPD) and SPE method, using two representative lipid standards, PC 14:0/14:0 and PE 15:0/15:0.

In the positive ion mode, when compared to the classic B&D method, G/TiO_2 method retained well, the phospholipid ions with higher signal response and removed the ions of non-phospholipid such as DAG, TAG, and their fragments (Fig. 3A and B as shown before). In the zoomed m/z range of 470–570 (Figs. S2A and B), ion $[LPE20:3+H]^+$ (m/z 504.4) was obviously detected by G/TiO_2 method but not by the B&D method. Moreover, with this new method, ions intensity of m/z 520.3, 542.3, 544.3 were markedly increased. For the traditional B&D method, the signals of phospholipids in the MALDI mass spectra are suppressed by the glycerol ions due to the in-source competition of ionization, which has been long regarded as one of the biggest obstacles for the specific quantitative evaluation of phospholipids in the MALDI mass spectra. The eluent obtained from the washing step of SPE were further subjected to MALDI-TOF analysis, and were found out to be glycerides. It means that, in comparison with the traditional B&D method, the G/TiO_2 could efficiently fortify the absorption of the phospholipids and remove the glycerol compounds by the washing step.

In the negative ion mode, no significant difference could be observed between the mass spectra of B&D method and G/TiO_2 method (Fig. 4A and B as shown before) at first glance. However,

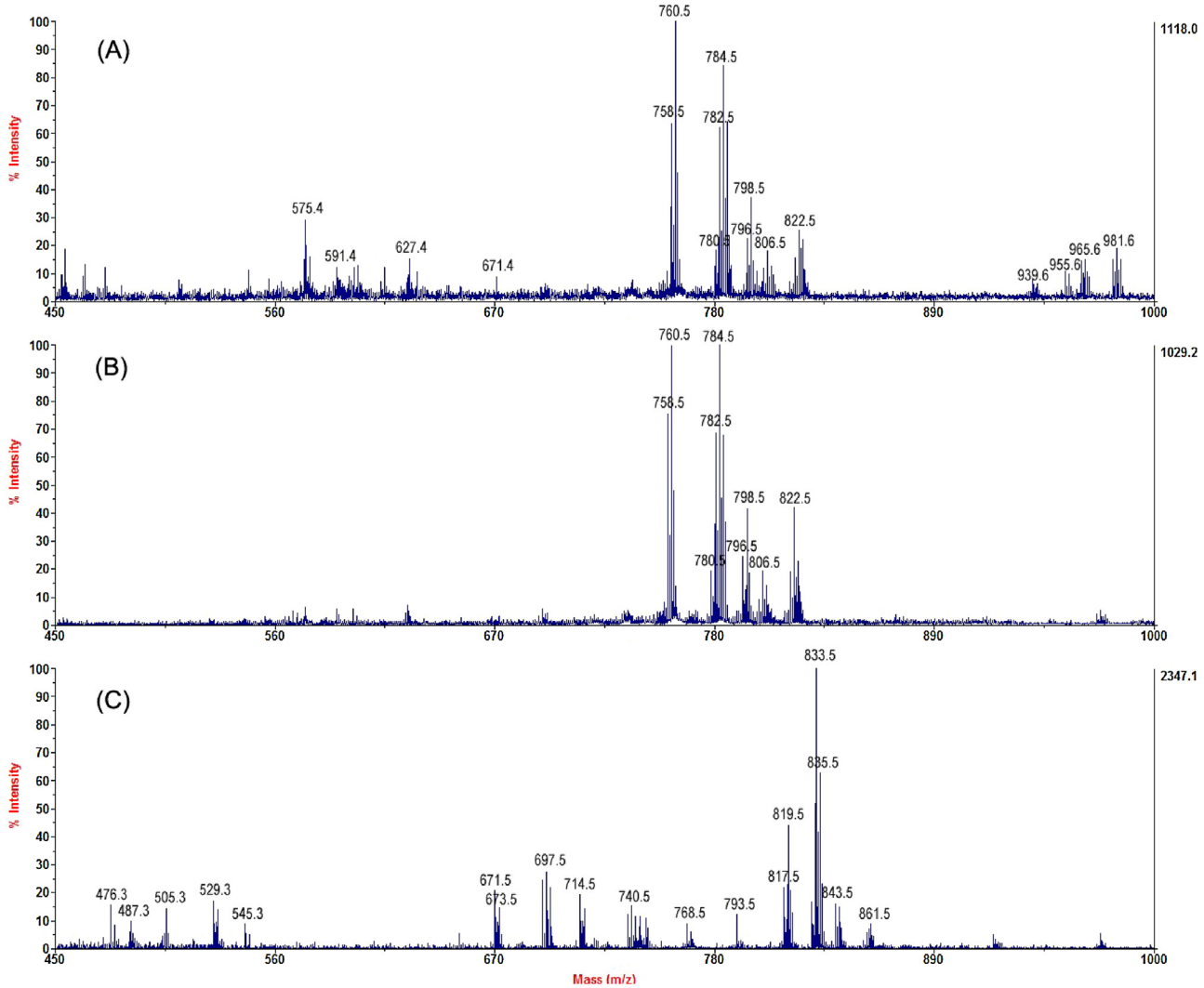

Fig. 5. Positive MALDI-TOF/MS spectra relevant to (A) B&D extracts and (B) G/TiO_2 based SPE extracts of avocado seed sample. Negative MALDI-TOF/MS spectra relevant to (C) G/TiO_2 based SPE extracts of avocado seed sample.

further investigation showed that great amount of noises were reduced when G/TiO_2 based SPE was applied to purify phospholipids. The *m/z* range of 470–510 of Fig. 4A and B were zoomed and shown in Fig. S2C and D, respectively. The reduced noise could be observed more obviously. Some peaks of lysophospholipids, such as $[LPC16:0+H]^+$ (*m/z* 496.3), were enhanced, indicating the effectiveness of G/TiO_2 in selective extraction of phospholipids.

The performance of three methods (G/TiO_2 SPE, TiO_2 MSPD and TiO_2 SPE) were compared using enrichment factor (EF), which was defined as the ratio between the concentration of the analyte in the final eulate and the concentration of the analyte in the solution applied to the proposed three methods. The results are summarized in Table S3. The highest EF of PC and PE were 2.97 and 3.03, respectively, obtained by G/TiO_2 SPE method. For TiO_2 SPE method, because the bed of SPE cartridge was easily collapsed when TiO_2 was directly used as SPE sorbent, the loading capacity of TiO_2 SPE cartridge reduced, leading to comparatively lower EFs (EF_{PC} 0.61 and EF_{PE} 0.67). The lowest EFs were obtained by TiO_2 MSPD method (EF_{PC} 0.05 and EF_{PE} 0.05). It indicated that MSPD method can be used for extraction and purification, but is not suitable for enrichment. Meanwhile, MSPD cartridge is dispotable and cannot be reused. Therefore, G/TiO_2 based SPE is proven to be an ideal method for selective extraction of phospholipids.

3.4. Method application and data analysis

PCA was applied to data analysis of the 88 avocado samples, including the pulps and seeds. Fig. 6 shows the PC1 and PC2 plot of avocado samples that explained 76.8% of total variance of the dataset. The dataset of MALDI-TOF/MS spectra from the pulps and seeds of avocado samples demonstrated a good clustering of replicates. As shown in Fig. 6A, the clusters are well separated by the PC1 axis, and the intra-cluster variation could be explained by the PC2 axis. The cluster on the left side represents the seeds while that on the right side represents the pulps. Examination of the loadings plot (Fig. 6B) revealed the most influential ions that is responsible for separation between clusters. The ions which had the greatest influence on the scores plot were those farthest away from the main cluster of ions. Examination of PC1 loadings showed that sample variability between pulps and seeds could be attributed to many ions. For example, *m/z* 786.5 ($[PC18:0/18:2+H]^+$/$[PC18:1/18:1+H]^+$), *m/z* 760.5 ($[PC16:0/18:1+H]^+$), and *m/z* 845.6 ($[PI\ O\text{-}18:1/18:2-H]^-$) were the dominant features with loading values of 0.52, 0.33, and 0.33, respectively. In fact, the contents of these ions could be regarded as the major difference between the pulps and seeds. In addition, the ions responsible for intra-cluster variation could be observed from the PC2 axis of loading plot. For instance, the loading value of *m/z* 760.5 ($[PC16:0/18:1+H]^+$) was as high as 0.8, meaning that the content of PC16:0/18:1 varied greatly in different pulp samples. Meanwhile, the loading values of *m/z* 784.5 ($[PC18:1/18:2+H]^+$) and *m/z* 786.5 ($[PC18:0/18:2+H]^+$/$[PC18:1/18:1+H]^+$) were also high, indicating the individual differences of avocado samples. As a conclusion, the PCA results revealed the major difference between the pulp and seed samples, that is the contents of ions with high absolute PC1 loading value and low absolute PC2 loading value, like *m/z* 845.6 ($[PI\ O\text{-}18:1/18:2-H]^-$).

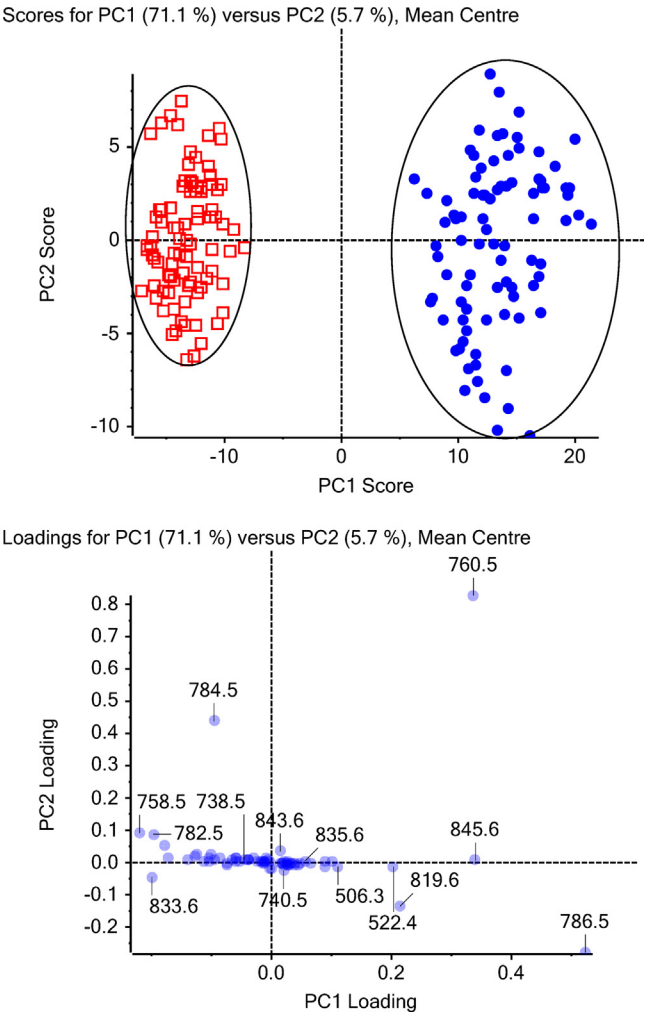

Fig. 6. Principal component analysis of the identified phospholipid species of avocado pulp and seed samples.

4. Conclusion

In this study, a strategy for extraction and analysis of phospholipids was developed and applied to both avocado pulps and seeds. G/TiO_2 was synthesized and packed in SPE cartridge for selective extraction of phospholipids from crude lipid mixture. Meanwhile, a MALDI-TOF/MS technique was utilized in both positive and negative ion modes for analysis of the sample eluent. The experimental conditions involved in sample preparation and analyses were optimized. Then, this strategy was successfully applied to avocado pulps and seeds. The interfering glycerides were efficiently removed, resulting in a clean spectra of phospholipids. All the ions detected were characterized and submitted to PCA statistical analysis, which revealed the major difference between pulp and seed samples. In conclusion, the optimized G/TiO_2 based SPE method combined with MALDI-TOF/MS analysis is an efficient, reliable and easy procedure to selectively extract and study phospholipids in avocado samples.

Conflict of interest

The authors declare no competing financial interest.

Acknowledgments

The authors thank the Hong Kong Chinese Materia Medica Standards (HKCMMS) Fund (CityU Project No. 9211024) from the Department of Health, Hong Kong SAR Government and Internal Research Matching Fund (No. 7002872) from the City University of Hong Kong. Qing Shen, Mei Yang and Linqiu Li also thank the

financial support from the Research Grants Council (RGC) of Hong Kong for giving them studentships to do a PhD degree in City University of Hong Kong.

Appendix A. Supplementary data

Supplementary data associated with this article can be found, in the online version, at http://dx.doi.org/10.1016/j.aca.2014.09.022.

References

[1] V.M. Gomez-Lopez, Characterization of avocado (*Persea americana* Mill.) varieties of low oil content, J. Agric. Food. Chem. 47 (1999) 2707–2710.
[2] M. Gondwe, D.R. Kamadyaapa, M.A. Tufts, A.A. Chuturgoon, J.A. Ojewole, C.T. Musabayane, Effects of *Persea americana* Mill. (*Lauraceae*) ["Avocado"] ethanolic leaf extract on blood glucose and kidney function in streptozotocin-induced diabetic rats and on kidney cell lines of the proximal (LLCPK1) and distal tubules (MDBK), Methods Find. Exp. Clin. Pharmacol. 30 (2008) 25–35.
[3] Q.Y. Lu, J.R. Arteaga, Q. Zhang, S. Huerta, V.L. Go, D. Heber, Inhibition of prostate cancer cell growth by an avocado extract: role of lipid-soluble bioactive substances, J. Nutr. Biochem. 16 (2005) 23–30.
[4] A.J. Butt, C.G. Roberts, A.A. Seawright, P.B. Oelrichs, J.K. Macleod, T.Y. Liaw, A novel plant toxin, persin, with in vivo activity in the mammary gland, induces Bim-dependent apoptosis in human breast cancer cells, Mol. Cancer Ther. 5 (2006) 2300–2309.
[5] H. Kawagishi, Y. Fukumoto, M. Hatakeyama, P. He, H. Arimoto, T. Matsuzawa, Liver injury suppressing compounds from avocado (*Persea americana*), J. Agric. Food Chem. 49 (2001) 2215–2221.
[6] E.R. Eckhardt, D.Q. Wang, J.M. Donovan, M.C. Carey, Dietary sphingomyelin suppresses intestinal cholesterol absorption by decreasing thermodynamic activity of cholesterol monomers, J. Gastroenterol. 122 (2002) 948–956.
[7] S. Chen, C. Liu, Ether glycerophospholipids and their potential as therapeutic agents, Curr. Org. Chem. 17 (2013) 802–811.
[8] H. Gallart-Ayala, F. Courant, S. Severe, J.-P. Antignac, F. Morio, J. Abadie, B. Le Bizec, Versatile lipid profiling by liquid chromatography–high resolution mass spectrometry using all ion fragmentation and polarity switching. Preliminary application for serum samples phenotyping related to canine mammary cancer, Anal. Chim. Acta 796 (2013) 75–83.
[9] R. Sutphen, Y. Xu, G.D. Wilbanks, J. Fiorica, E.C. Grendys, J.P.J. LaPolla, H. Arango, M.S. Hoffman, M. Martino, K. Wakeley, D. Griffin, R.W. Blanco, A.B. Cantor, Y. Xiao, J.P. Krischer, Lysophospholipids are potential biomarkers of ovarian cancer, Cancer Epidemiol. Biomarkers Prev. 13 (2004) 1185–1191.
[10] C. Wang, H. Kong, Y. Guan, J. Yang, J.R. Gu, S.L. Yang, G.W. Xu, Plasma phospholipid metabolic profiling and biomarkers of type 2 diabetes mellitus based on high-performance liquid chromatography/electrospray mass spectrometry and multivariate statistical analysis, Anal. Chem. 77 (2005) 4108–4116.
[11] R. Katz-Bull, D. Seger, D. Rivenson-Segal, E. Rushkin, H. Degani, Metabolic markers of breast cancer: enhanced choline metabolism and reduced choline–ether–phospholipid synthesis, Cancer Res. 62 (2002) 1966–1970.
[12] I.D. van der Werf, C.D. Calvano, F. Palmisano, L. Sabbatini, A simple protocol for matrix assisted laser desorption ionization-time of flight-mass spectrometry (MALDI-TOF-MS) analysis of lipids and proteins in single microsamples of paintings, Anal. Chim. Acta 718 (2012) 1–10.
[13] S.S. Bird, V.R. Marur, M.J. Sniatynski, H.K. Greenberg, B.S. Kristal, Lipidomics profiling by high-resolution LC–MS and high-energy collisional dissociation fragmentation: focus on characterization of mitochondrial cardiolipins and monolysocardiolipins, Anal. Chem. 83 (2011) 940–949.
[14] S. Chen, N.A. Belikova, P.V. Subbaiah, Structural elucidation of molecular species of pacific oyster ether amino phospholipids by normal-phase liquid chromatography/negative-ion electrospray ionization and quadrupole/multiple-stage linear ion-trap mass spectrometry, Anal. Chim. Acta 735 (2012) 76–89.
[15] Q. Shen, Y. Wang, L. Gong, R. Guo, W. Dong, H.Y. Cheung, Shotgun lipidomics strategy for fast analysis of phospholipids in fisheries waste and its potential in species differentiation, J. Agric. Food Chem. 60 (2012) 9384–9393.
[16] P. Lucci, D. Pacetti, I. Calzuola, V. Marsili, S. Perni, F. Giavarini, N.G. Frega, G.L. Gianfranceschi, Characterization of phospholipid molecular species and peptide molecules in wheat sprout hydroalcoholic extract, J. Agric. Food Chem. 61 (2013) 11453–11459.
[17] E. Boselli, D. Pacetti, P. Lucci, N.G. Frega, Characterization of phospholipid molecular species in the edible parts of bony fish and shellfish, J. Agric. Food Chem. 60 (2012) 3234–3245.
[18] Q. Liu, J. Shi, J. Sun, T. Wang, L. Zeng, G. Jiang, Graphene and graphene oxide sheets supported on silica as versatile and high-performance adsorbents for solid-phase extraction, Angew. Chem. 123 (2011) 6035–6039.
[19] M.R. Larsen, T.E. Thingholm, O.N. Jensen, P. Roepstorff, T.J.D. Jorgensen, Highly selective enrichment of phosphorylated peptides from peptide mixtures using titanium dioxide microcolumns, Mol. Cell. Proteomics 4 (2005) 873–886.
[20] G.T. Cantin, T.R. Shock, S.K. Park, H.D. Madhani, J.R. Yates, Optimizing TiO_2-based phosphopeptide enrichment for automated multidimensional liquid chromatography coupled to tandem mass spectrometry, Anal. Chem. 79 (2007) 4666–4673.
[21] Q. Shen, W. Dong, M. Yang, J.T. Baibado, Y. Wang, I. Alqouqa, H.Y. Cheung, Lipidomic study of olive fruit and oil using TiO_2 nanoparticle based matrix solid-phase dispersion and MALDI-TOF/MS, Food Res. Int. 54 (2013) 2054–2061.
[22] Q. Shen, W. Dong, M. Yang, L. Li, Y. Wang, H.Y. Cheung, Z. Zhang, Lipidomic fingerprint of almonds (*Prunus dulcis* L. cv Nonpareil) using TiO_2 nanoparticle based matrix solid-phase dispersion and MALDI-TOF/MS and its potential in geographical origin verification, J. Agric. Food Chem. 61 (2013) 7739–7748.
[23] K. Engholm-Keller, M.R. Larsen, Titanium dioxide as chemo-affinity chromatographic sorbent of biomolecular compounds – applications in acidic modification-specific proteomics, J. Proteomics 75 (2011) 317–328.
[24] D.C. Marcano, D.V. Kosynkin, J.M. Berlin, A. Sinitskii, Z. Sun, A. Slesarev, L.B. Alemany, W. Lu, J.M. Tour, Improved synthesis of graphene oxide, ACS Nano 4 (2010) 4806–4814.
[25] Y. Liang, H. Wang, H.S. Casalongue, Z. Chen, H. Dai, TiO_2 nanocrystals grown on graphene as advanced photocatalytic hybrid materials, Nano Res. 3 (2014) 701–705.
[26] D. Touboul, S. Roy, D.P. Germain, A. Baillet, F. Brion, P. Prognon, P. Chaminade, O. Laprévote, Fast fingerprinting by MALDI-TOF mass spectrometry of urinary sediment glycosphingolipids in Fabry disease, Anal. Bioanal. Chem. 382 (2005) 1209–1216.
[27] M. Preianò, L. Pasqua, L. Gallelli, O. Galasso, G. Gasparini, R. Savino, R. Terracciano, Simultaneous extraction and rapid visualization of peptidomic and lipidomic body fluids fingerprints using mesoporous aluminosilicate and MALDI–TOF MS, Proteomics 12 (2012) 3286–3294.
[28] S. Harrabi, W. Herchi, H. Kallel, P.M. Mayer, S. Boukhchina, Liquid chromatographic–mass spectrometric analysis of glycerophospholipids in corn oil, Food Chem. 114 (2009) 712–716.